# Water structures at metal electrodes studied by ab initio molecular dynamics simulations

Axel Groß[a,b], Florian Gossenberger[a], Xiaohang Lin[a], Maryam Naderian[a], Sung Sakong[a], and Tanglaw Roman[a]
[a] *Institute of Theoretical Chemistry, Ulm University, 89069 Ulm, Germany*
[b] *Helmholtz Institute Ulm (HIU) Electrochemical Energy Storage, 89069 Ulm, Germany*
(Dated: February 3, 2014)

The structure of water on metal electrodes is addressed based on first-principles calculations. Special emphasis is paid on the competition between water-metal and water-water interaction as the structure determining factors. Thus the question will be discussed whether water at metal surfaces is ice- or rather liquid-like. The proper description of liquid phases requires to perform thermal averages. This has been done by combining first-principles electronic structure calculations with molecular dynamics simulations. After reviewing recent studies about water on flat, stepped and pre-covered metal electrodes, some new results will be presented.

Keywords: electrochemistry, density functional theory

## I. INTRODUCTION

Structures and processes at electrochemical interfaces between a solid electrode and a liquid electrolyte are of great technological importance [1, 2], for example in electrochemical energy conversion and storage, electrocatalysis, corrosion, or even in the preparation of organic layers used in molecular electronic devices, just to name a few. Besides, solid-liquid interfaces are of fundamental interest [3–5] since they represent the boundary between an ordered and an disordered phase. Still, our knowledge of the atomistic structure of these interfaces and its consequences on their properties and function is rather limited.

This is partially due to the fact that some of the experimental tools with microscopic resolution that have been used so successfully at the solid-vacuum interface are not available for the solid-liquid interface. Hence experiments often do not yield a detailed atomistic information but rather integrated or average quantities. This is in part a consequence of the very nature of the liquid phase. Since it corresponds to a disordered phase, there is no fixed atomic structure that can be exactly measured so that necessarily only thermally averaged atomic distributions can be derived. Hence often even a continuous modeling is still performed in which the liquid phase is represented by a continuum characterized by a dielectric constant [6].

With respect to the structure of the electrode-water interface, there have been numerous molecular dynamics studies addressing solid-water interfaces at finite temperatures using parameterized interaction potentials. While these classical potentials might reproduce structural properties of the water quite satisfactorily [7–9], the interaction between the substrate, typically metals, and the water molecules is not described reliably since there is no interpolation scheme that can describe covalent bonding *and* hydrogen bonding *and* metal bonding at the same time.

On the other hand, periodic electronic structure calculations based on density functional theory (DFT) within the generalized gradient approximation (GGA) for the treatment of exchange-correlation effects have become a reliable tool to address water-metal interfaces since they can yield a satisfactory description of both the water-water interaction and the water-metal interaction [10]. Based on periodic DFT calculations, *ab initio* molecular dynamics (AIMD) simulations in which the forces necessary to integrate the classical equations of motion are computed "on the fly" by first-principles electronic structure calculations can be performed [11, 12]. This method allows an appropriate statistical sampling of possible structures and processes at solid-liquid interfaces from first principles, i.e. without using semi-empirical parameterized interaction potentials. In addition, it provides information on the underlying electronic structure thus making a proper analysis of chemical trends possible.

For biological and aqueous systems, the AIMD technique is well-established [13, 14], in particular using the Car-Parrinello scheme [15] based on density functional theory (DFT) which is well-suited for systems with a non-vanishing band gap. These AIMD simulations have provided deep insights into dynamical processes in complex systems such as the proton migration in water [14]. For processes at surfaces, in particular metal surfaces, the AIMD technique had been rarely used [16–18] because of the high computational demand. This situation has now changed due to the ever increasing computer power and the development of more efficient algorithms [12]. In two seminal works more than one decade ago, Izvekov and coworkers addressed the structure of the water-Cu(110) [19] and the water-Ag(111) [20] interface by AIMD simulations. Only recently this work was taken up [21–23] in order to elucidate the structure of electrode-water interfaces. It has been shown that it is possible to run a satisfactory number of AIMD trajectories for sufficiently long times in order to obtain meaningful statistical results in molecule-surface interactions [12, 24, 25].

In this work, we will first discuss recent AIMD studies addressing the structure of water on flat, stepped and pre-covered metal surfaces. Evidence will be provided that the structure of water at close-packed metal sur-

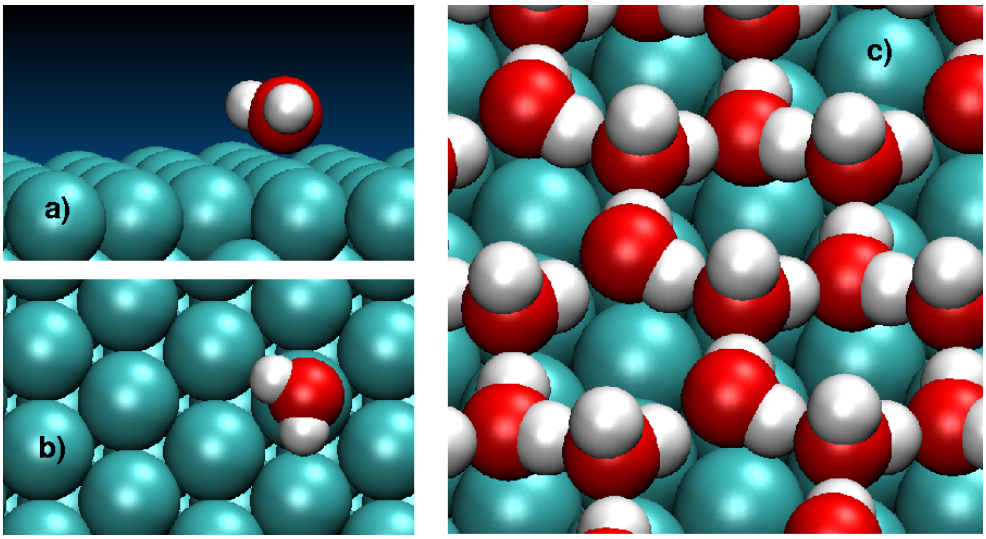


FIG. 1. Water adsorbed on a fcc(111) metal electrode. a, b) Side and top view of a single adsorbed water molecule, c) ice-like hexagonal H-up water bilayer.

faces is rather liquid- than ice-like. Comparing different systems, the role of the water-water and the water-metal interaction on the structure of water at metal electrodes will be discussed. Finally, some new AIMD results of water structures at pre-covered surfaces will be presented.

## II. COMPUTATIONAL DETAILS

All AIMD simulations shown in this paper were performed using periodic DFT calculations. Most of the presented calculations were done using the Vienna ab initio program package (VASP) [26]. Electron-core interactions were accounted for by the projector augmented wave method [27, 28]. The electronic one-particle wave functions were expanded in a plane-wave basis set up to an energy cutoff of 500 eV. Exchange-correlation effects were described using the functional of Perdew, Burke, and Ernzerhof (PBE) [29]. Furthermore, studies using the revised PBE functional (RPBE) by Hammer *et al.* [30] will also be presented. In addition, the role of van der Waals forces will be discussed using DFT calculations with semi-empirical dispersion corrections [31].

The AIMD simulations shown in this work were typically run for about 10 ps within the microcanonical ensemble by solving the classical equation of motions with the help of the Verlet algorithm [31] with a time step of 1 fs.

## III. RESULTS AND DISCUSSION

We will first address the geometric structure of water at the water-metal interfaces according to DFT calculations. As a starting point, we consider the adsorption of a single water molecule on a flat metal (111) electrode. Single water molecules typically bind via their oxygen atom to the top sites of metal surfaces in an almost flat configuration, as illustrated in Fig. 1 a and b, at distances between 2.25 Å (Cu) and 3.02 Å (Au) from the metal atoms [10]. These relative large distances are a consequence of the relatively weak binding of water monomers to metal surfaces. For typical late transition metals, the interaction strength is ordered according to Au<Ag<Cu<Pd<Pt<Ru<Rh with adsorption energies ranging from -0.1 eV to -0.4 eV [10].

As far as the formation of water layers on metal surfaces is concerned, it is important to note that water forms a hydrogen-bonded network. The water-water interaction is of comparable strength or even stronger than the water-metal interaction. On closed-packed hexagonal metal surfaces, the energetically most favorable structures correspond to a water bilayer [10, 32] whose structure is similar to that of the densest layer of ice [3]. In this particular structure, every second water molecule binds with its oxygen atom to the metal surface similar to the water monomer shown in Fig. 1b. For the other water molecules, there are in fact two different possible orientations, namely the so-called H-down and H-up structures with one hydrogen atom either pointing towards or away from the surface. The H-up structure is illustrated in Fig. 1c. These hexagonal water structures are stable on fcc metals such as Cu(111), Pt(111) and Au(111) for which the lattice constants vary by about 15%. This shows that the hydrogen-bonded water network is relatively flexible with respect to changes in the lattice constant.

In order to understand the structure formation of water on hexagonal metal electrodes, it is of interest to decompose the computed adsorption energies in the bilayer

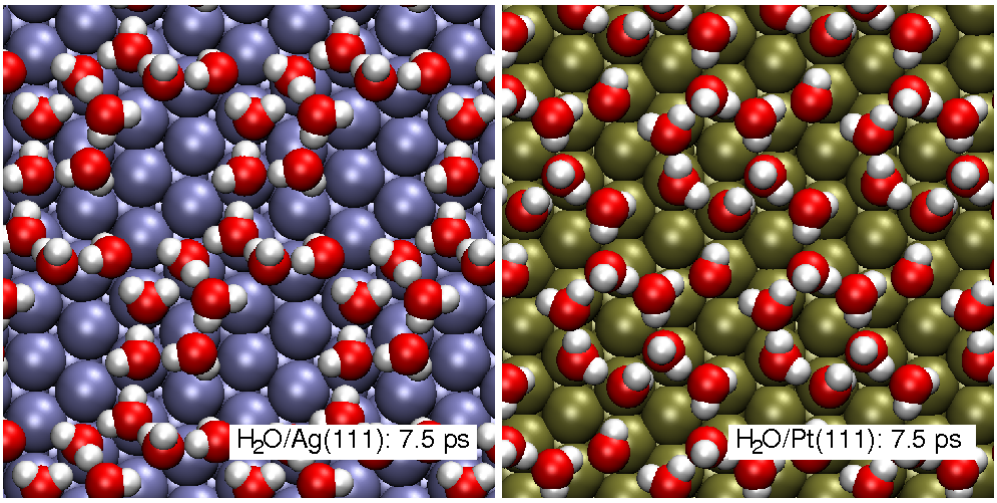


FIG. 2. Snapshots of AIMD simulations of two water layers on Ag(111) and Pt(111) at 300 K. Only the first water layer is shown [22].

structures into the contribution from the water-metal and the water-water interaction. There are two ways to regard the structure formation [10, 32]. One can assume that the bilayer is first assembled in the gas phase and then deposited onto the electrode surface. Alternatively, first the water molecules are adsorbed individually on the surface and then assembled into the ice-like bilayer structure. The first approach assumes that the inter-water binding during the adsorption of the water bilayer remains unchanged whereas the second approach ignores that the water-metal interaction might change when the water bilayer is formed. This means that there is no unique way to decompose the water adsorption energies into the two contributions.

As a consequence, using the two energy decomposition schemes describe above leads to different results [10, 32]. Still, the differences are rather small, as we illustrate using the adsorption of a water bilayer on the bimetallic overlayer system Pd/Au(111) as an example. The adsorption energy of the water layer with respect to the free water molecule amounts to -0.53 eV per water molecule [32] whereas the adsorption energy with respect to a free water bilayer is only -0.12 eV. This means that most of the energy gain upon the formation of the water bilayer of the metal overlayer is due to the water-water interaction, and the water-metal interaction is reduced with respect to the adsorption of a single water molecule. Similar results have also been found for electrodes made of other transition metals [10].

The studies discussed so far were all concerned with energy minimum structures of water on fcc(111) metal electrodes. Yet, the question arises whether at room temperature ice-like structures on fcc(111) electrodes are really stable or whether rather liquid-like structures occur. In order to address this question thermal averages have to be performed which require a high numerical effort. Since both the water-water and the water-metal interaction has to be described properly, numerically favorable classical molecular dynamics (MD) simulations based on force fields are not really suited. Fortunately, due to the ever-increasing computer power and the development of more efficient algorithms first-principles simulations of complex structures and processes at surfaces [33] and the combination of MD simulations with first-principles electronic structure calculations have become possible.

Izvekov and co-workers were the first to address the structure of water layers on metal surfaces with AIMD simulations. They studied the structure of water on Cu(110) [19] and on Ag(111) [20] at room temperature. However, for both systems no hexagonal surface unit cells were used so that the thermal stability of the hexagonal ice-like layer could not be assessed.

Later, in a systematic study the structure of two water layers on Ag(111), Au(111), Pt(111), Pd/Au(111) and Ru(0001) at room temperature were studied using AIMD simulations [22]. Fig. 2 shows snapshots of the AIMD trajectories of water on Ag(111) and Pt(111). The simulations were started with the ice-like bilayer as the initial configuration. As Fig. 2 demonstrates, for water on Ag(111) after 7.5 ps no indication of the initial hexagonal geometry is left, the structure is disordered, there is some clustering and most of the water molecules bind via their oxygen atom to the substrate. For water on Pt(111), on the other hand, there is still a hexagonal geometry visible. This structure might be an artefact of the relatively small $2\sqrt{3}\times 2\sqrt{3}$ unit cell, but still a higher lateral order than on Ag(111) is observed. Yet, there is no indication of either the H-up or the H-down structure left, the orientation of the water molecules is disordered.

Note that the work function change of the metal electrodes upon water adsorption strongly depends on the orientation of the water molecules, the H-up and H-

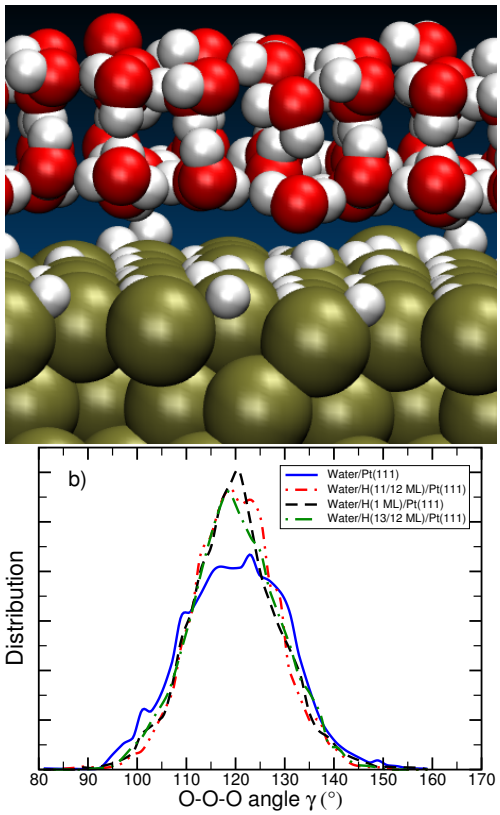


FIG. 3. Water on hydrogen-covered Pt(111). a) Snapshot of a AIMD trajectory of two water layers on hydrogen-covered Pt(111) at room temperature, b) distribution of the O-O-O angle of water on clean and hydrogen-covered Pt(111) along AIMD trajectories [34].

down structure cause work function changes that differ by about 2 eV because of their opposite dipole orientation [22, 23, 35]. Furthermore, neither the H-up structure nor the H-down structure yield work function changes [23] that agree with experimental findings for Au(111) [36], Pt(111) [37, 38] or Ru(0001) [39, 40]. In fact, the experimentally found work functions for these systems lie in between the calculated ones for the H-up and H-down structures. Only if the thermal motion of the water molecules is taken into account in the simulations, experimental and theoretical results become consistent [22, 23] because then the preferential orientation of the water molecules and thus of their dipole moments is significantly reduced. This gives strong evidence that indeed water layers at close-packed fcc(111) electrodes are disordered at room temperature.

Still, Fig. 2 yields qualitative differences with respect to the degree of disorder, water on the noble metal surface Ag(111) is also laterally disordered whereas on the more strongly interacting Pt(111) electrode still a hexagonal ordering exists. This might imply that the hexagonal ordering of the water layer is a consequence of the interaction between metal electrode and water. With respect to water on Pt(111) it should be noted, however, that under electrochemical conditions at low potentials the Pt(111) electrode becomes hydrogen-covered [41, 42].

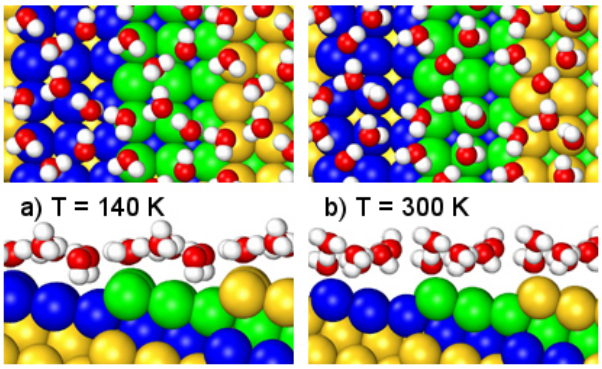


FIG. 4. Top and side views of snapshots of a AIMD run of a water layer on Au(511) at a) $T = 140\,\mathrm{K}$ and b) $T = 300\,\mathrm{K}$ [43].

The presence of a hydrogen adlayer on Pt(111) has severe consequences on the resulting water structures, as was shown using AIMD simulations at room temperature [34]. Figure 3a shows a snapshot of an AIMD simulation of two water layers on hydrogen-covered Pt(111). The adsorption of hydrogen on Pt(111) leads to a passivation of the Pt-electrode. The strength of the water-metal interaction is significantly reduced which results in a distance of the water layer from the Pt atoms which is increased by about 1 Å compared to clean Pt(111). However, not only the distance is increased, also the order within the water-layers is increased. In Fig. 3b, the distribution in the O-O-O angle along the AIMD trajectories for water on clean Pt(111) and hydrogen-covered Pt(111) with different hydrogen coverages close to unity is plotted. For a perfect ice-like structure, this distribution would be peaked at 120°, the width of the distribution is thus a descriptor of the deviation from a perfect ice-like structure. And indeed, the distributions on hydrogen-covered Pt(111) are more peaked than the distribution on clean Pt(111).

This suggests that a weaker metal-water interaction causes a stronger order in the water layer. This can be rationalized by the fact that a weaker metal-water interaction leads to a stronger water-water interaction in the water bilayer which stabilizes the water hydrogen-bonded network. However, this seems to be at variance to the AIMD findings for water on Ag(111) where a weaker water-metal interaction causes a reduced order in the water layer.

In this context it is interesting to consider the structure of a water layer on stepped noble metal surfaces. In Fig. 4, snapshots of a AIMD simulation of water on Au(511) at $T = 140\,\mathrm{K}$ and $T = 300\,\mathrm{K}$ are shown [43]. This system was studied by vibrational spectroscopy by Ibach [44]. Based on the vibrational spectra Ibach made a suggestion for the structure of a water layer on Au(511) which was confirmed to be an energy minimum structure

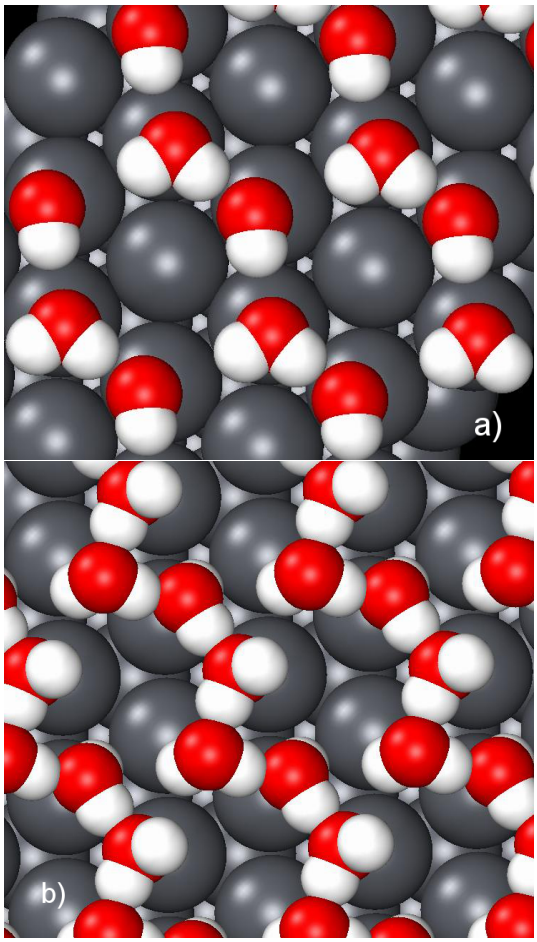


FIG. 5. Energy minimum structure of a hexagonal water layer on Pb(111) for water coverages of a) $\Theta_{H_2O} = 2/3$ and b) $\Theta_{H_2O} = 1$.

in the DFT calculations [43]. It consists of an arrangement of the water network in tetragons, hexagons and octagons (see Fig. 4a). Furthermore, the measured vibrational spectra could also be confirmed in the AIMD simulations which allow to derive vibrational spectra through the Fourier transform of the velocity auto-correlation function.

Interestingly enough, this water network remained relatively stable also after 10 ps in the room temperature run (see Fig. 4b) whereas on Au(111) the water network was already dissolved after 8 ps. The side view of the water structure on Au(511) in Fig. 4 reveals that the oxygen atoms of the water molecules approximately form a flat layer which is only bound through the oxygen atoms above the step atoms. This picture is confirmed by an analysis of the charge density difference upon water adsorption [43]. Thus the water layer is pinned to the metal step atoms whereas the water molecules above the small (100)-like terrace are not directly bound to the metal substrate. This again leads to a stronger water-water interaction which apparently stabilizes the water network.

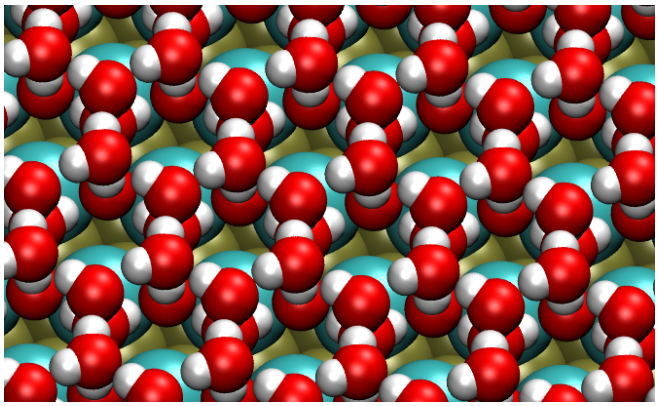

FIG. 6. Structure of two water bilayers on a $\sqrt{3}\times\sqrt{3}$ chlorine-covered Pt(111).

The particular water structure on Au(511) which is indeed also found to be the most stable on Ag(511) obviously results as a compromise between the creation of the hydrogen-bonded network and the best-suited arrangement on the stepped (511) surface. Apparently, the surface structure matters as far as the network formation is concerned. This is also obvious if one tries to form a hexagonal ice-like water layer on Pb(111) whose lattice constant of 4.95 Å is much larger than those of, e.g., the late transition metals. Figure 5a shows the calculated energy minimum structure within this arrangement corresponding to a water coverage of $\Theta_{H_2O} = 2/3$. It is apparent that the Pb-Pb distance is already too large to form a real hexagonal hydrogen-bonded network, there is a large variation on the O-H separation of the hydrogen bonds. The structure rather corresponds of an arrangement of water dimers. This is also reflected in the low adsorption energy of -0.254 eV with respect to the free water molecule which is significantly lower than the corresponding adsorption energies on Au(111) and Ag(111).

In fact, the energy gain per water molecule in creases to -0.350 eV for a higher coverage of $\Theta_{H_2O} = 1$, the resulting energy minimum structure is illustrated in Fig. 5b. Note that still no real two-dimensional water network results, the water layer rather corresponds to an arrangement of water chains. Consequently, the binding energy per water molecule is still less than the binding energies in the hexagonal structure on the late transition metals.

With respect to the electrochemical interface between a metal electrode and an aqueous electrolyte it is also important to note that in an acid environment usually specific adsorption of anions occurs [1, 2, 45, 46]. As far as the adsorption of halides is concerned, typical coverages are in the range of $0.33 - 0.45$ [45–50]. The presence of such a relatively high coverage of anions of course also has a significant impact on the water structure on metal electrodes. Figure 6 illustrates the structure of two water bilayers on a $\sqrt{3} \times \sqrt{3}$ chlorine-covered Pt(111) surface corresponding to a chlorine coverage of $\Theta_{Cl} = 1/3$. It is clearly visible that at such a high halide coverage the low-

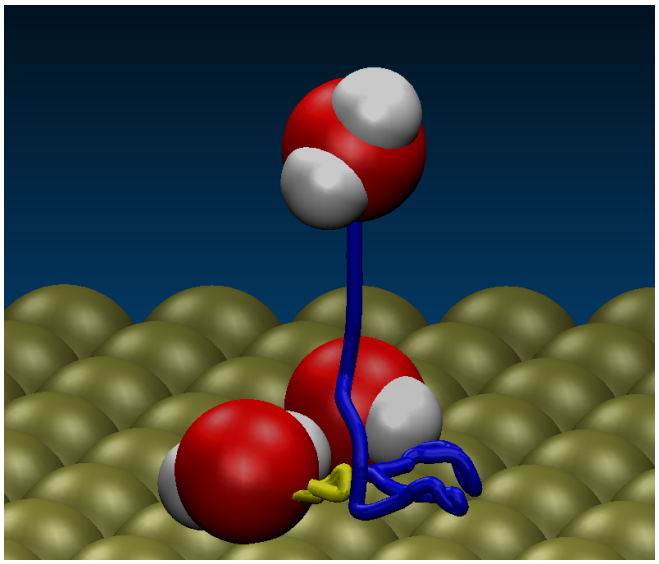

FIG. 7. Initial and final configuration plus the traces of the oxygen atoms of a water molecules impinging on Pt(111) (initial kinetic energy $E_{\mathrm{kin}} = 50\,\mathrm{meV}$) with an adsorbed water molecule already present, determined by AIMD simulations within a $3 \times 3$ geometry. The periodic images of the water molecules are omitted for the sake of clarity.

est water layer is not directly interacting with the metal electrode but rather located above the halide layer. Furthermore, it should be noted that such an adsorbate layer can have a poisoning effect on the catalytic activity of the electrode [51, 52].

AIMD simulations can also been used to dynamical details of adsorption processes [25], such as the initial steps of the formation of the hydrogen-bonded network of water on metal electrodes. Figure 7 illustrates the trajectory of a water molecule that impinges on a Pt(111) surface with an initial kinetic energy $E_{\mathrm{kin}} = 50\,\mathrm{meV}$ within a $3\times4$ geometry where already a water molecule is present. The binding energy of the water dimer is about 0.2 eV, as on other surfaces [32] or in the gas phase [53]. Trajectories of water molecules with different orientations and impact points within a $3 \times 3$ unit cell were started, and in all studied cases the water dimer forms spontaneously. This means that water molecules impinging close to an adsorbed water molecule will be steered [54] towards to it and form the initial configuration of a water network. This also means that the energy gain of about 0.2 eV will be effectively dissipated to the substrate and the molecular degrees of freedom.

Still, a further problem arises as far as the DFT description of water-based electrolytes is concerned. Liquid water described by popular DFT functionals such as the PBE functional [29] is over-structured (see, e.g., [55–57]) which is reflected in the fact that the peaks in the radial distribution function are too pronounced. This problem is related to the fact that the directional hydrogen-bonding is overestimated by the PBE functional. As a way out, it has been suggested to perform DFT-PBE simulations of liquid water at higher temperatures [55–57], which is, however, an unsatisfactory solution.

Another possible way to correct this erroneous description is to replace directional H-bonds by non-directional van der Waals forces [58–60]. Current DFT exchange-correlation functionals do not appropriately reproduce the long-range van der Waals or dispersion interaction. We propose to use the RPBE functional [61] together with semi-empirical dispersion corrections [31] which are computationally inexpensive. Recently we were able to show that using the RPBE functional [61] together with semi-empirical dispersion corrections [31] within a RPBE-D approach the wetting behavior of water on close-packed metal surfaces can be correctly reproduced [53] which is not possible using either PBE, PBE-D or pure RPBE calculations.

It should still be mentioned that although AIMD simulations of processes and structures at interfaces can nowadays be routinely performed, they still are associated with a considerable numerical effort. This effort can be significantly reduced if the water layer is represented by an implicit solvent model [6]. Still, the validity of implicit solvent models has to be carefully assessed. We have started to use a recent implementation of such a model [62] into the VASP code. First results indicate that the reduction of hydrogen binding energies on metal surfaces in the presence of water [32, 63] is reproduced when the explicit water layer is replaced by the implicit description. In addition, we modeled water layers above the metal electrodes by combining one explicitly water bilayer with the implicit water description. We found that the H-down configuration on Pt(111) becomes unstable in the presence of the implicit water model. Whereas there is hardly any attractive interaction between the hydrogen atom of the H-down water molecule and the Pt electrode, for the opposite orientation there is a favorable interaction with the implicit water model. Further properties will be tested in our ongoing work.

## IV. CONCLUSIONS

The structure of water at metal electrodes has been discussed based on ab initio molecular dynamics simulations. On strongly interacting close-packed metal electrodes and on very weakly interacting metal substrates still some lateral order in the water arrangement has been found. This can be interpreted as being due to the structure of the electrode imposed onto the water in the first case of the strongly interacting substrate or as being due to the strong water-water interaction stabilizing the hydrogen-bonded water network in the second case of the weakly interacting substrate. For an intermediate interaction strength as for substrates such as Au(111) or Ag(111) no lateral order in the water layer is present any more. This suggests that in these cases neither the water-metal nor the water-water interaction is strong enough in

order to stabilize the hexagonal water network.

However, it might well be that the run time of the AIMD simulations presented here of about 10 ps might still be too short to give final conclusions about the structure at thermal equilibrium but this only applies to those structures which still show some order. In any case, there is hardly any orientational order of the water molecules at room temperature which is confirmed by the water-induced work-function change that assumes intermediate values between those for the ice-like H-up and H-down bilayers.

While these considerations apply to water layers on close-packed (111) electrodes, more complex substrate structures including co-adsorbates or steps can significantly influence the structure of water layers, as we have illustrated using either hydrogen- or chlorine-covered Pt(111) and Au(511) as examples. Such studies are a first step towards the more realistic modeling of water/electrode interfaces, as they occur, e.g., in electrocatalysis. Ab initio molecular dynamics simulations combining reliable first-principles electronic structure calculations with molecular dynamics simulations are a suitable tool to address such solid/liquid interfaces.

## ACKNOWLEDGMENTS

This research has been supported by the German Science Foundation (DFG) through the research unit FOR 1376 (DFG contract GR 1503/21-1) and by the Baden-Württemberg Foundation within the Network of Excellence *Functional Nanostructures*. Computer time has been provided by the BW-Grid of the federal state of Baden-Württemberg and by a computer cluster financed through the stimulus programme "Electrochemistry for Electromobility" of the German Ministry of Education and Science (BMBF).

[1] W. Schmickler, Chem. Rev. **96**, 3177 (1996).
[2] R. Guidelli and W. Schmickler, Electrochim. Acta **45**, 2317 (2000).
[3] P. A. Thiel and T. E. Madey, Surf. Sci. Rep. **7**, 211 (1987).
[4] M. A. Henderson, Surf. Sci. Rep. **46**, 1 (2002).
[5] A. Hodgson and S. Haq, Surf. Sci. Rep. **64**, 381 (2009).
[6] A. Klamt, J. Phys. Chem. **99**, 2224 (1995).
[7] J. I. Siepmann and M. Sprik, J. Chem. Phys. **102**, 511 (1995).
[8] P. S. Crozier, R. L. Rowley, and D. Henderson, J. Chem. Phys. **113**, 9202 (2000).
[9] R. Bukowski, K. Szalewicz, G. C. Groenenboom, and A. van der Avoird, Science **315**, 1249 (2007).
[10] A. Michaelides, Appl. Phys. A **85**, 415 (2006).
[11] D. Marx and J. Hutter, Ab initio molecular dynamics: Theory and implementation, in *Modern Methods and Algorithms of Quantum Chemistry*, edited by J. Grotendorst, volume 3 of *NIC series*, pages 329–477, John von Neumann-Institute for Computing, Jülich, 2000.
[12] A. Groß and A. Dianat, Phys. Rev. Lett. **98**, 206107 (2007).
[13] P. Carloni, U. Rothlisberger, and M. Parrinello, Acc. Chem. Res. **35**, 455 (2002).
[14] D. Marx, ChemPhysChem **7**, 1848 (2006).
[15] R. Car and M. Parrinello, Phys. Rev. Lett. **55**, 2471 (1985).
[16] A. De Vita, I. Štich, M. J. Gillan, M. C. Payne, and L. J. Clarke, Phys. Rev. Lett. **71**, 1276 (1993).
[17] A. Groß, M. Bockstedte, and M. Scheffler, Phys. Rev. Lett. **79**, 701 (1997).
[18] L. C. Ciacchi and M. C. Payne, Phys. Rev. Lett. **92**, 176104 (2004).
[19] S. Izvekov, A. Mazzolo, K. Van Opdorp, and G. A. Voth, J. Chem. Phys. **114**, 3284 (2001).
[20] S. Izvekov and G. A. Voth, J. Chem. Phys. **115**, 7196 (2001).
[21] M. Otani, I. Hamada, O. Sugino, Y. Morikawa, Y. Okamoto, and T. Ikeshoji, Phys. Chem. Chem. Phys. **10**, 3609 (2008).
[22] S. Schnur and A. Groß, New J. Phys. **11**, 125003 (2009).
[23] S. Schnur and A. Groß, Catal. Today **165**, 129 (2011).
[24] A. Groß, Phys. Rev. Lett. **103**, 246101 (2009).
[25] A. Groß, J. Chem. Phys. **135**, 174707 (2011).
[26] G. Kresse and J. Furthmüller, Phys. Rev. B **54**, 11169 (1996).
[27] P. E. Blöchl, Phys. Rev. B **50**, 17953 (1994).
[28] G. Kresse and D. Joubert, Phys. Rev. B **59**, 1758 (1999).
[29] J. P. Perdew, K. Burke, and M. Ernzerhof, Phys. Rev. Lett. **77**, 3865 (1996).
[30] B. Hammer, L. B. Hansen, and J. K. Nørskov, Phys. Rev. B **59**, 7413 (1999).
[31] S. Grimme, J. Antony, S. Ehrlich, and H. Krieg, J. Chem. Phys. **132**, 154104 (2010).
[32] A. Roudgar and A. Groß, Chem. Phys. Lett. **409**, 157 (2005).
[33] A. Groß, Surf. Sci. **500**, 347 (2002).
[34] T. Roman and A. Groß, Catal. Today **202**, 183 (2013).
[35] J. S. Filhol and M.-L. Bocquet, Chem. Phys. Lett. **438**, 203 (2007).
[36] J. M. Heras and L. Viscido, Appl. Surf. Sci. **4**, 238 (1980).
[37] E. Langenbach, A. Spitzer, and H. Lüth, Surf. Sci. **147**, 179 (1984).
[38] M. Kiskinova, G. Pirug, and H. Bonzel, Surf. Sci. **150**, 319 (1985).
[39] W. Hoffmann and C. Benndorf, Surf. Sc. **377-379**, 681 (1997).
[40] Y. Lilach, L. Romm, T. Livneh, and M. Asscher, J. Phys. Chem. B **105**, 2736 (2001).
[41] T. J. Schmidt, P. N. Ross Jr., and N. M. Markovic, J. Electroanal. Chem. **524**, 252 (2002).
[42] N. M. Marković and P. N. Ross Jr., Surf. Sci. Rep. **45**, 117 (2002).
[43] X. Lin and A. Groß, Surf. Sci. **606**, 886 (2012).
[44] H. Ibach, Surf. Sci. **604**, 377 (2010).
[45] O. M. Magnussen, Chem. Rev. **107**, 679 (2002).
[46] D. V. Tripkovic, D. Strmcnik, D. van der Vliet, V. Stamenkovic, and N. M. Markovic, Faraday Discuss. **140**,

25 (2009).
[47] P. Broekmann, M. Wilms, M. Kruft, C. Stuhlmann, and K. Wandelt, J. Electroanal. Chem. **467**, 307 (1999).
[48] B. Obliers, P. Broekmann, and K. Wandelt, J. Electroanal. Chem. **554-555**, 183 (2003).
[49] Y. Gründer, A. Drünkler, F. Golks, G. Wijts, J. Stettner, J. Zegenhagen, and O. M. Magnussen, Surf. Sci. **605**, 1732 (2011).
[50] F. Gossenberger, T. Roman, and A. Groß, Surf. Sci. **630** (2014).
[51] C. M. Wei, A. Groß, and M. Scheffler, Phys. Rev. B **57**, 15572 (1998).
[52] A. Groß, Surf. Sci. **608**, 249 (2013).
[53] K. Tonigold and A. Groß, J. Comput. Chem. **33**, 695 (2012).
[54] A. Groß, Surf. Sci. **363**, 1 (1996).
[55] M. V. Fernández-Serra and E. Artacho, J. Chem. Phys. **121**, 11136 (2004).
[56] J. VandeVondele, F. Mohamed, M. Krack, J. Hutter, M. Sprik, and M. Parrinello, J. Chem. Phys. **122**, 014515 (2005).
[57] L.-M. Liu, M. Krack, and A. Michaelides, J. Chem. Phys. **130**, 234702 (2009).
[58] A. Møgelhøj, A. K. Kelkkanen, K. T. Wikfeldt, J. Schiøtz, J. J. Mortensen, L. G. M. Pettersson, B. I. Lundqvist, K. W. Jacobsen, A. Nilsson, and J. K. Nørskov, J. Phys. Chem. B **115**, 14149 (2011).
[59] C. Zhang, J. Wu, G. Galli, and F. Gygi, J. Chem. Theory Comput. **7**, 3054 (2011).
[60] I.-C. Lin, A. P. Seitsonen, I. Tavernelli, and U. Rothlisberger, J. Chem. Theory Comput. **8**, 3902 (2012).
[61] B. Hammer, L. B. Hansen, and J. K. Nørskov, Phys. Rev. B **59**, 7413 (1999).
[62] K. Mathew, R. Sundararaman, K. Letchworth-Weaver, T. A. Arias, and R. G. Hennig, subm. to J. Chem. Phys. , http://arxiv.org/abs/1310.4242, 2013.
[63] A. Roudgar and A. Groß, Surf. Sci. **597**, 42 (2005).